Adsorbate Structures from Photoelectron Diffraction: Holographic Reconstruction or Real-Space Triangulation?

R. Dippel,(1) D. P. Woodruff,(2) X.-M. Hu,(2) M. C. Asensio,(2),(a) A. W. Robinson,(1),(b)
K.-M. Schindler,(1) K.-U. Weiss,(1) P. Gardner,(1) and A. M. Bradshaw(1)
(1)*Fritz Haber Institute, Faradayweg 4-6, D-1000 Berlin 33, Germany*
(2)*Physics Department, University of Warwick, Coventry CV4 7AL, United Kingdom*

(Received 23 December 1991)

By preselecting the appropriate photoelectron energies with the aid of simple model calculations, we show that the main peaks in angular distributions of core-level photoemission from adsorbed species on surfaces, caused by elastic backscattering, can be directly related to adsorbate-substrate interatomic directions, thus permitting direct real-space triangulation of adsorption sites on surfaces. The method is demonstrated with the aid of experimental data from oxygen and CO on Cu(110), and offers comparable spatial resolution to holographic inversion, but requires a much smaller data set.

PACS numbers: 61.14.−x, 68.35.Bs, 79.60.Gs

Recently there has been considerable interest in the idea that the angular distribution of photoelectrons emitted from a solid surface, caused by coherent interference between the directly emitted electron wave field and components elastically scattered by surrounding atoms, can be viewed as a photoelectron hologram (e.g., Refs. [1-3] and references therein). This description has led to the suggestion that a measured photoelectron diffraction "pattern" can be mathematically inverted to provide an atomic resolution "image" of the emission site (i.e., that an image can be reconstructed from the hologram). Furthermore, there have been several publications concerned with attempts to overcome some of the problems of this inversion associated with scattering phase shifts, multiple scattering, and nonspherical wave fronts. Although there has been some progress in developing such methods, which have been tested mainly using simulated experimental data, it seems clear that the precision (and possibly the accuracy) may be no better than ±0.5 Å even in favorable cases, and may involve amassing considerable amounts of experimental data (e.g., complete angular distributions at ten or more distinct photoelectron energies).

In the past, experiments aimed at exploiting photoelectron diffraction for the determination of surface and near-surface structures have concentrated on one of two rather different experimental conditions [4]. At relatively high photoelectron energies (typically 500-1000 eV or greater) the dominant elastic scattering processes are in the near-forward direction and the photoemission flux peaks in directions corresponding to emitter-scatterer bond directions (e.g., Refs. [5-7]). Under these conditions valuable structural information on the location of atoms lying *above the emitter* can be obtained rather directly from the identification of these real-space directions, and the technique is valuable for the study of adsorbed molecule orientation, and for investigating the structure of thin epitaxial overlayers. At lower energies (typically 50-400 eV) *backscattering* intensities are sufficient to produce significant photoelectron diffraction effects, *and allow determination of the location of adsorbed atoms relative to the underlying substrate atoms* (e.g., Refs. [8-15]). This structural analysis is normally achieved with the aid of model calculations for trial structures. The inefficiency of this trial and error approach to structure determination is one of the principle attractions of the holographic inversion, even if it is imprecise, because it provides a *direct* route to an approximate solution which can then be refined by existing methods. We show here, however, that by proper choice of the photoelectron energies, angular photoemission distributions in backscattering geometries can be used to obtain adsorbate bonding directions directly by real-space triangulation. This represents a simpler method than holographic inversion and offers comparable, if not better, spatial resolution.

Our basic starting point is the observation that in low-energy photoelectron diffraction from adsorbed atoms, the strongest effects due to diffraction usually occur in emission directions for which a near-neighbor substrate scatterer lies almost directly behind the emitter relative to the collector (i.e., having a scattering angle close to 180°). This effect has been noted by us [11-16] in many adsorbate structure studies using photoelectron diffraction and appears to be due, at least in part, to the peaking of the backscattering cross section which occurs at 180° at most energies. Second, we note that for the great majority of adsorption systems of interest, the nearest-neighbor adsorbate-substrate bond length can be reliably estimated to within better than ±0.1 Å, without any experiment, simply on the basis of interatomic bond lengths in appropriate compounds, or by taking the sum of appropriate atomic (covalent) radii. It is therefore extremely simple to calculate, for such a system, the two-atom energy-dependent 180° backscattering spectrum; i.e., the photoemission flux which would be measured along the scatterer-emitter (substrate-adsorbate) direction if a scanned-energy-mode photoelectron diffraction experiment were to be performed on a hypothetical oriented molecule of these two atomic species. This spec-

© 1992 The American Physical Society

trum has a simple damped periodic form,

$$I = I_0\{1 + A(k)\cos[2kr + \phi(k,\pi)]\}\ ,$$

in which k is the photoelectron wave number, r is the emitter-scatterer separation, A is a backscattering amplitude in which the main k dependence is damping with increasing k, and $\phi(k,\pi)$ is the 180° (π) backscattering phase shift which is readily calculable from atomic potentials. The important feature of this calculated spectrum is that the peaks correspond to the energies at which the backscattering is exactly in phase with the directly emitted flux along the interatomic bond length. This means that an angular distribution of the photoemitted flux measured at such an energy shows a peak in the real-space interatomic bond direction. Conversely, an angular distribution recorded at an energy corresponding to a minimum in this spectrum will show a dip along the interatomic bond direction. This simple phenomenon provides the basis of our method.

Figure 1 provides a schematic illustration of this backscattering experiment which is compared with the high-energy forward scattering situation. Note that in the forward scattering case the peak in the photoemission flux along the interatomic direction is a zero-order diffraction feature [the path-length difference between the reference and scattering paths is zero, and the scattering phase shift $\phi(k,0)$ is small ($\ll \pi$)]; weak first- and higher-order diffraction peaks occur at other emission angles. By contrast, in the backscattering case, the diffraction peak along the interatomic direction is nth order (n depending on the energy and thus the photoelectron wavelength) while the subsidiary peaks are of order $n-1$, $n-2$, etc. Figure 1 also shows the results of model calculations for both the energy dependence of the photoemitted flux from an initial s state in a two-atom (emitter-scatterer) cluster along the two-atom axis, and the angular dependence at selected energies corresponding to minima and maxima in the energy-scanned spectrum; these theoretical results are from simple single scattering ("curved wave") calculations in which the scattering atom is Cu and the emitter-scatterer separation is 2.0 Å. Clearly, the results of these simple calculations support the idea that a dominant photoemission angular peak or minimum can be obtained along the backscattering nearest-neighbor direction (polar angle 0°) by the appropriate preselection of photoelectron energy. Notice that there is a systematic error in the location of this main feature of some 5° which arises from the symmetry-breaking effect of the incident x-ray polarization vector (the calculation assumes the linearly polarized radiation is incident at 60° relative to the collector, and the sample is rotated to obtain the angle-scan data). The main angular feature is also broad, such that a total error in locating the peak of up to 10° is possible; this would lead, over the 2-Å spacing, to an error in locating the backscatterer of some 0.4 Å, comparable to the errors of the best holographic reconstructions claimed so far.

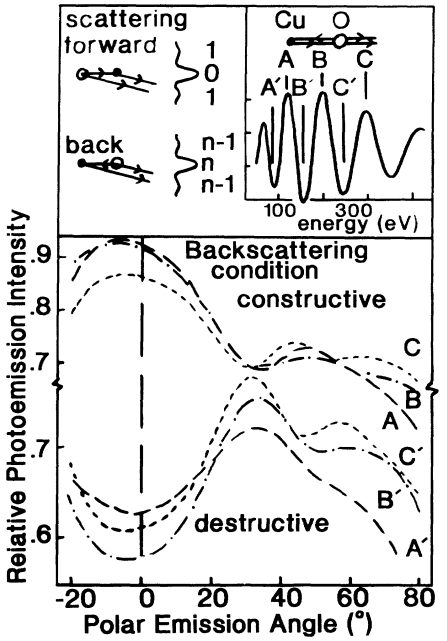

FIG. 1. Illustration of the basic idea of the backscattering photoelectron diffraction angle-scan experiment. In the upper left is shown schematically the high-energy forward scattering, and general energy backscattering, photoelectron interference paths and the resulting angular distributions with the diffracted orders labeled. The graph in the upper right shows the calculated scanned-energy-mode photoelectron diffraction spectrum for 180° backscattering from a Cu atom 2.0 Å behind the emitter. The lower graph shows polar angle scans from this two-atom emission system calculated at the energies corresponding to the maxima and minima of the axial direction scanned-energy-mode spectrum.

One potential problem in applying these ideas which is not evident in the results of these simple two-atom calculations is the role of other scattering atoms when the emitter is placed on the surface of a real, extensive, solid. In the high-energy forward scattering experiment the strong forward peaking of the scattering cross section ensures that angular scans are dominated by zero-order forward scattered peaks. At intermediate energies in the backscattering geometry, the backscattering peak in the scattering cross section is far less pronounced, and in a general emission direction many scatterers can contribute. The consequence of this, readily tested with simple scattering cluster calculations, is that angular scans from an emitter adsorbed on an extended solid surface, recorded at energies chosen to enhance the role of the nearest-neighbor substrate scatterers as described above, do always show main features (peaks or minima) attributable to these nearest neighbors, but also show other structure which can, in some cases, be similar in magnitude. However, the *systematic* appearance of the predicted nearest-neighbor features in all such angular scans suggests a simple solution to this problem. If one evaluates the *ratio* of the photoemitted intensities in angular scans collected at photoelectron energies corresponding to constructive and destructive interference along the nearest-neighbor bond direction, the resulting angular scan should become dominated by the nearest-neighbor contributions because in the nearest-neighbor directions this procedure consistently divides local maxima by local minima. Other features will not generally produce similarly correlated effects at the two energies, and so will be suppressed in the ratio.

In order to demonstrate the viability of these ideas we have carried out experimental investigations of two model adsorption systems for which the structures are reasonably well known, namely, atomic oxygen and molecular CO on Cu(110). The Cu(110)(2×1)-O phase investigated here has been extensively studied by a variety of methods and is clearly established [13,17–19] to involve a missing (added) row reconstruction with the oxygen atoms occupying long bridge sites. These oxygen atoms are quite close to coplanar with the top Cu atom layer, although there is some controversy about the exact value of this top O-Cu layer spacing. The oxygen atoms occupy short bridge sites relative to the second-layer Cu atoms, and the nearest-neighbor Cu atoms in this layer therefore lie on interatomic vectors at 39° from the surface normal in the ⟨110⟩ azimuth at a distance generally accepted to be close to 2.0 Å (see Fig. 2). In the case of CO on Cu(110), vibrational spectroscopy [20] indicates atop adsorption as on the other low-index faces of Cu, and while no previous quantitative structural study exists for the Cu(110)/CO system, similar studies of CO adsorption on Cu(100) indicate a Cu-C nearest-neighbor distance close to 1.9 Å [21,22].

The experiments were conducted in a purpose-built ultrahigh-vacuum spectrometer system taking soft x radiation from the BESSY electron storage ring through the Fritz Haber Institute's HE-TGM monochromator. The Cu(110) sample was prepared by the usual methods and was dosed with oxygen at room temperature and with CO at liquid nitrogen temperature. A VG Scientific 100-mm-mean-radius 150° electrostatic deflection analyzer (having three parallel detectors) was installed at a fixed angle of 60° relative to the photon incidence direction. The O and C 1*s* photoemission peaks were scanned at a series of polar emission angles, varied by rotating the crystal in a ⟨110⟩ azimuth so that the incidence direction relative to the crystal also varies. Each of these photoemission energy spectra was then fitted numerically to achieve background subtraction, and the integrated areas were plotted as a function of polar emission angle. Photoelectron energies were chosen to be close to those anticipated to coincide with ideal nearest-neighbor scattering constructive or destructive interference along the interatomic axis as described above. The two-atom calculation for a Cu-emitter separation of 2 Å given in Fig. 1 is well suited to the chemisorbed oxygen, while the optimum energies for C 1*s* from CO adsorption are slightly higher, corresponding to the slightly smaller (1.9 Å) anticipated Cu-C bond length.

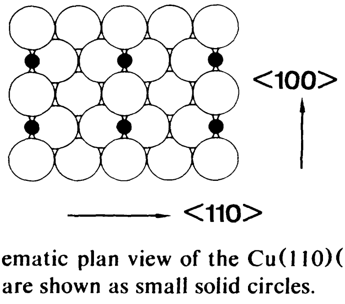

FIG. 2. Schematic plan view of the Cu(110)(2×1)-O structure. O atoms are shown as small solid circles.

Figure 3 shows O 1*s* photoemission polar-angle-scan data from the chemisorbed oxygen on Cu(110) recorded at photoelectron energies corresponding fairly closely to the maxima and minima of the two-atom spectrum of Fig. 1 labeled *B* and *B*′. The nearest-neighbor Cu atoms lie behind the emitter at a polar angle of 39° (Fig. 2), and these raw polar angle plots provide some support for our proposed simple interpretation in that the *B* plot shows a major peak around 33° and the *B*′ plot shows a broad minimum at this angle. A similar pair of polar angle scans recorded from the C 1*s* photoemission peak for CO adsorbed on Cu(110) are shown in the upper part of Fig. 4. In this case, the backscattering peak is expected along the surface normal, and is seen in data recorded in

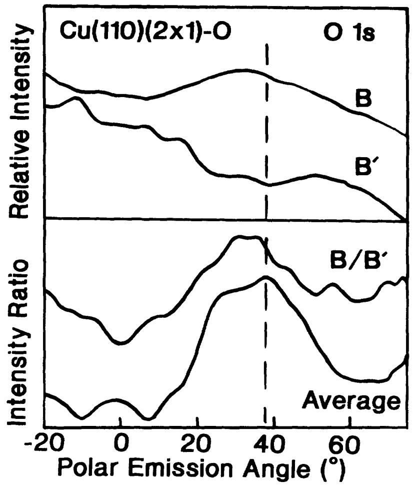

FIG. 3. Experimental O 1*s* photoemission angle scans recorded in the ⟨110⟩ azimuth from Cu(110)(2×1)-O. The upper part of the figure shows the raw angular scans at photoelectron energies close to those corresponding to the *B* maximum and *B*′ minimum of the two-atom calculation of Fig. 1; the actual experimental energies were 150 and 204 eV. The lower part shows intensity ratios of these data, and of an average of ratios corresponding approximately to the conditions *A*/*B*′, *B*/*B*′, and *B*/*C*′.

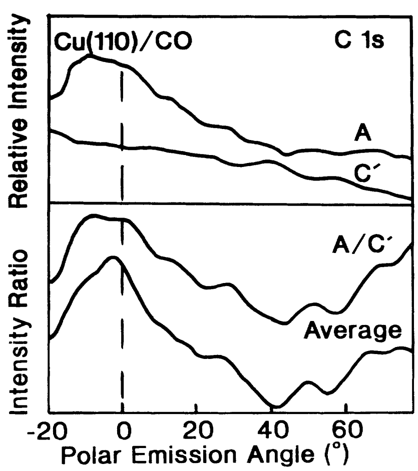

FIG. 4. Experimental C $1s$ photoemission angle scans recorded in the ⟨110⟩ azimuth from CO adsorbed on Cu(110). The format is similar to that of Fig. 3, but the experimental photoelectron energies used were A, 132 eV and C', 280 eV. The average is derived from the ratios A/C', A/B', B/C', and C/C'.

the constructive scattering condition A, while a weak minimum is found at the destructive condition C'. Taking the maximum to minimum ratios leads to a clear broad peak around the appropriate bond directions. The systematic shift of the experimental peak to a smaller angle than the true interatomic direction, by a few degrees, is consistent with the polarization vector effect identified in the simple calculations of Fig. 1. Polar scans recorded at other energies show similar trends, but with varying fine structure; the systematic behavior, however, revealed in an average of several constructive-to-destructive intensity ratios, shows the predicted peak along the backscattering bond direction very clearly, as shown by the lowest curves of Fig. 3 and 4.

These two examples serve to illustrate the potential of our method for obtaining the essential adsorption geometry from polar angle scans of backscattered photoelectron diffraction data. Armed with a prior estimate of the adsorbate-substrate bond length, a simple calculation identifies the photon energies at which polar scans should be recorded. By recording at least two such scans corresponding to constructive and destructive interference along an interatomic axis one can determine the interatomic bond angle and thus the nearest-neighbor substrate atom location to within a few tenths of an angstrom unit. Structural refinement can then be achieved using normal photoelectron diffraction methods with the aid of full model calculations. Even though it may be necessary generally to record polar scans in several azimuths, the number of data points required is still much smaller than is currently perceived necessary for holographic inversion, and the method of interpretation is much simpler.

The authors are pleased to acknowledge the financial support of the Science and Engineering Research Council (United Kingdom), the European Commission (SCIENCE programme), and the German Federal Ministry for Research and Technology for research grants which have made this work possible.

---

[a] Present address: Instituto de Ciencia de Materiales, Consejo Superior de Investigaciones Cientificas, Serrano 144, 28006 Madrid, Spain.

[b] Present address: Surface Science Research Centre, University of Liverpool, Liverpool L69 3BX, United Kingdom.

[1] J. J. Barton, Phys. Rev. Lett. **61**, 1345 (1988).
[2] D. K. Saldin, G. R. Harp, B. L. Chen, and B. P. Tonner, Phys. Rev. B **44**, 2480 (1991).
[3] H. Huang, H. Li, and S. Y. Tong, Phys. Rev. B **44**, 3240 (1991).
[4] D. P. Woodruff, in "Angle Resolved Photoemission," edited by S. D. Kevan (Elsevier, Amsterdam, to be published).
[5] L.-G. Petersson, S. Kono, N. F. T. Hall, C. S. Fadley, and J. B. Pendry, Phys. Rev. Lett. **42**, 1545 (1979).
[6] W. F. Egelhoff, Jr., Phys. Rev. B **30**, 1052 (1984).
[7] S. A. Chambers, S. B. Anderson, and J. H. Weaver, Phys. Rev. B **32**, 581 (1985).
[8] D. P. Woodruff, D. Norman, B. W. Holland, N. V. Smith, H. H. Farrell, and M. M. Traum, Phys. Rev. Lett. **41**, 1130 (1978).
[9] S. D. Kevan, D. H. Rosenblatt, D. R. Denley, B.-C. Lu, and D. A. Shirley, Phys. Rev. Lett. **41**, 1565 (1978).
[10] J. J. Barton, S. W. Robey, and D. A. Shirley, Phys. Rev. B **34**, 778 (1986).
[11] D. P. Woodruff, C. F. McConville, A. L. D. Kilcoyne, Th. Lindner, J. Somers, M. Surman, and A. M. Bradshaw, Surf. Sci. **201**, 228 (1988).
[12] Th. Lindner, J. Somers, A. M. Bradshaw, A. L. D. Kilcoyne, and D. P. Woodruff, Surf. Sci. **203**, 333 (1988).
[13] A. W. Robinson, J. S. Somers, D. E. Ricken, A. M. Bradshaw, A. L. D. Kilcoyne, and D. P. Woodruff, Surf. Sci. **227**, 237 (1990).
[14] M. C. Asensio, M. J. Ashwin, A. L. D. Kilcoyne, D. P. Woodruff, A. W. Robinson, Th. Lindner, J. S. Somers, D. E. Ricken, and A. M. Bradshaw, Surf. Sci. **236**, 1 (1990).
[15] A. L. D. Kilcoyne, D. P. Woodruff, A. W. Robinson, Th. Lindner, J. S. Somers, and A. M. Bradshaw, Surf. Sci. **253**, 107 (1991).
[16] A. L. D. Kilcoyne, D. P. Woodruff, Th. Lindner, J. Somers, and A. M. Bradshaw, J. Vac. Sci. Technol. A **7**, 1926 (1989).
[17] A. L. D. Kilcoyne, D. P. Woodruff, A. Robinson, Th. Lindner, J. Somers, D. E. Ricken, and A. M. Bradshaw, Faraday Discuss. Chem. Soc. **89**, 311 (1990); also references cited in this paper, and discussion on pp. 203–205.
[18] M. Bader, A. Puschmann, C. Ocal, and J. Haase, Phys. Rev. Lett. **57**, 3273 (1986).
[19] S. R. Parkin, H. C. Zeng, M. Y. Zhou, and K. A. R. Mitchell, Phys. Rev. B **41**, 5432 (1990).
[20] D. P. Woodruff, B. E. Hayden, K. Prince, and A. M. Bradshaw, Surf. Sci. **123**, 397 (1982).
[21] S. Andersson and J. B. Pendry, Phys. Rev. Lett. **43**, 363 (1979).
[22] C. F. McConville, D. P. Woodruff, K. C. Prince, G. Paolucci, V. Chab, M. Surman, and A. M. Bradshaw, Surf. Sci. **166**, 221 (1986).